Estimation and Mapping of Land Surface Temperature From AATSR Images And GIS: A Case Study In Kolondieba-Tiendaga Basin In Sudano-Sahelian Climate, Mali

Daou I[1]., Mariko A[2]., Rasmus F[3]., Menenti M[4]., Kourosh K[5]., Maïga H B[6]., Maïga S.M[1].,

[1]. University of Bamako, Faculty of Science and Techniques (FAST), Mali
[2]. National Engineering school-Aberhamane Baba Touré of Bamako, Mali
[3]. University of Geography and Geology of Copenhague, Denmark
[4]. Delft University of Technology, Department and flesh, Remote Sensing optical and laser Remote sensing, Netherlands.
[5]. University of Cheickh Anta Diop (UCAD), Laboratory of Education and Research in Geomatics

Abstract:
The knowledge of the various terms which intervene in the energy balance of surface is essential at the same time for the hydrologists, the amenagists, the agronomists, the meteorologists, and the climatologists. The land surface temperature of the making ground left the key parameters of this assessment, plays a fundamental part in the processes of interaction hydrosphere-biosphere, atmosphere. It represents, the temperature of canopy of the vegetation for the covered zones of vegetation, and the temperature of canopy of the vegetation plus that of the surface of the ground, for the zones of scattered vegetation. While it represents the temperature of surface of the ground for the zones bar soil. This land surface temperature can be collected through two approaches: conventional approaches, and them approaches of remote sensingThe conventional methods make it possible to collect the temperature of surface of the ground starting from measurements of weather stations. On the other hand, the approaches of remote sensing make it possible, as for them, to estimate the land surface through the use of model of energy balance of surface. In this study, model SEBS was used on satellite data AATSR to estimate and mapping the land surface temperature, on the catchment area of Kolondièba-Tiendaga, in southern Mali zone. These results show values of land surface temperature between 303 and 296 (°K) for standard deviations of 2, 66 and 0, 945. These results are similar to those already found elsewhere, in West Africa with the same types given of satellite images AASTR

Keywords: Land surface Temperature, model SEBS, Mapping, watershed of Kolondieba-Tiendaga, Mali

1. Introduction

The knowledge of the space-time variation of the land surface temperature intervening in the energy assessment of surface is key information in the energy exchanges and matter between the surface of the ground and the atmosphere [1, 2, 3, 4, 6, 12, 17, 36,]. Indeed, the land surface temperature is an important parameter in the energy assessment of surface and plays an essential part in the processes of interaction between the hydrosphere-Biosphere-Atmosphere and the cycle of water. In addition, the follow-up of the transfers of mass and energy to the level of a surface is dominating for the integrated management of the water resources and vegetable. It is also necessary for the good comprehension of the hydrological systems, the ecological and climatic ecosystems, like with the follow-up and the forecast of their evolutions [7, 8,9,10, 11, 13, 14].Information on the land surface temperature represents for the bar soil the temperature of surface of the ground, while it represents for the dense zones of vegetations, the temperature of surface of canopy of the vegetation[4]. However, for the zones of scattered vegetation, it determines the temperature of canopy of the vegetation, and ground surfaces it [4,17,18,19] . Traditionally, the data of land surface temperature are collected starting from the weather stations.Today, with the development of technologies of observation of the ground, the remote sensing and the GIS appears like a tool privileged for the collection and the follow-up of parameters biophysics, in particular the land surface temperature, the evapotranspiration, the albedo, because providing related information's to the mass transfers, and in particular to the processes of evapotranspiration. Several research related to the problems of measurement and collection of these parameters through the use of the technology of the thermal infra-red remote sensing [28, 29, 37, 20, 21, 22, 24]. Thus, the land surface temperature collected starting from the satellite data can be used for the evaluation of the evapotranspiration, the water stress of the vegetation and the requirement out of water for the annual cultures through the use of model of energy assessments of surface. With the international scales, these tools for remote sensing and GIS are requested more and more for the collection and the cartography of the parameters biophysics, particularly, the albedo, emissivity, the temperature of surface, the evapotranspiration, and the evaporative fraction, etcOur study proposes to measure and chart the temperature of surface of the ground starting from satellite images AATSR of platform ENVISAT of the European space agency (ESA) by using model SEBS (Surface Energy Balance System) developed

by [16, 19, 20, 29, 30, 31] on the catchment area of Kolondièba-Tiendaga, in soudano-sahelian medium, in southern the Mali zone.

2. Materials and Method

2.1 Study area

The study relates to the catchment area (Kolondièba-Tiendaga) located in southern Mali zone between Longitudes and Latitudes 34 °W and 6, 82°W and 10,15°N and 11,08°N. This basin of a surface of 3050 km ², is under basin of the transborder basin of the Outlaw (Fig.1). It is localized on the upstream reservoir of Niger, to approximately 262 km of Bamako (capital of Mali), and is limited to North by the town of Kolondieba, in the South by the commune of Sibirila to the border of the Ivory Coast, in the East by the commune of Fakola and Bougoula, in the West by the commune of Garalo (circle of Bougouni). Its discharge system is in Tiendaga on the road of Fakola. Its physical Characteristics are given in Tableau1. The catchment area of Kolondièba-Tiendaga has a tropical climate of transition or Sudanese Southern climate, characterized by the one hot season alternation and dries (November-April) and one rain season (May-October) where the annual pluviometric average is higher 1000mm/an. The monthly average temperatures vary between 38° in May and 23° in December. The values of the relative humidity oscillate between 82% in August and 38% in February. The radiation is strong during all the year, where the values of the potential evapotranspiration remain important, with a maximum in May (161) (DNH, Mali, 1990). The geological substratum is consisted metamorphic and granitic rocks covered with washed tropical ferruginous grounds, hydromorphic grounds ferralitic, and grounds. The relief is dominated by plates upstream of the basin, plains in the center and hollows downstream whose altitude can vary between 315 and 390m. the vegetation is characterized by savannas raised and shrubby of herbaceous, mixed with annual cultures.

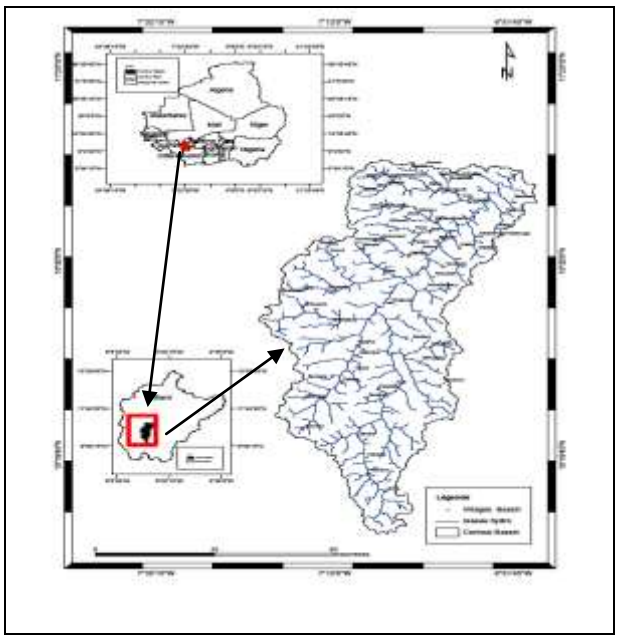

Figure 1: Presentation of the study area

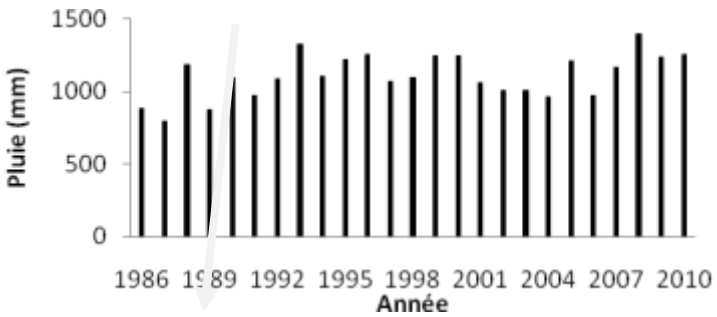

Figure2: Annual pluviometry recorded on the catchment area of Kolondièba-Tiendaga between 1986 and 2010

Tablel: Morphometric characteristics of the catchment area

Designation	Values
Discharge system	Longitudes : 11,066761 Latitudes : - 6,846652
Altitude discharge system	313 m
Surface basin	3050 Km^2
Length of the principal channel	158,30
The overall length of the hydrographic network	5854,26
Strahler order	7
Density of drainage	1,895km/Km^2
Perimeter	430 Km
Index of compactness	2,050 KG
Rectangle length equivalent	186 m
Largeur Rectangle equivalent	16m

2.2 Materials

The data of remote sensing used in this study are satellite images AATSR (Advanced Along Track Scanning Radiometer) of platform ENVISAT of the European space agency (ESA). Sensor AASTR is one of the six instruments of satellite ENVISAT launched by the European space agency, on March 1st, 2002 in polar orbit to provide data on the atmosphere, the ocean, the ground, and freezes it during the five next years. The data produced by ENVISAT will be exploited within the framework of the scientific research on the ground and the monitoring of the environmental and climatic changes. Moreover, they will facilitate the development of operational and commercial applications. Sensor AATSR is a radiometer with sweeping with a space resolution of 1Kmx1Km, recording 7 spectral bands in the visible one and the infra-red. The trace of sensor AATSR is selected in order to ensure a continuity with the data files of ATSR1 and ATSR2 of the series of ERS1 and ERS2 of ESA. The characteristics of the sensor are given in the tableau2. Products ATS-TOA level 1P of AATSR are used in this work. They were acquired near the European space agency (ESA) through the project of reinforcement of the capacities in Africa (TIGER II). These data were downloaded starting from the http://ats-merci-uk.eo.esa.int:8080/merci site, and relate to the period 2003 up to 2010. On the whole, we worked on more than 100 satellite images for the period quoted of in top (2003 up to 2010).

In addition to the satellite data, we used weather data obtained from National management of the Meteorology of Mali. They are relating to the temperature, the speed of the wind, the relative humidity. The data of solar radiation used in this work are collected in [35]

Table2: Characteristics of sensor AATSR of satellite ENVISAT (Esa, 2009)

Spectrales Bands spectrales (µm)	Central wavelength (µm)	Bandwidth (µm)	Spatial resolution (Km)	Application
0,0545-0,565	0,555	0,02	1	Chlorophyl
0549-0,669	0,659	0,02	1	Vegetation index
0,855-0,875	0,865	0,02	1	Vegetation index
1,580-1,640	1,61	0,03	1	Cleaning of cloud
3,50-3,89	3,70	0,30	1	Temperature of sea surface
10,40-11,30	10,85	1,00	1	Temperature of sea surface
11,50-12,50	12,00	1,00	1	Temperature of sea surface

As regards the geometrical resolution, sensor AATSR gathers these data according to two systems of curved sweepings:

A sweeping curved forwards (Forward curved scan)

A sweeping curved towards Nadir (Nadir curved scan)

2.3 Methods

The methodology used in this study is based on model SEBS (Surface Energy Balance System) developed the European space agency (ESA). This model was developed by [16,19,20, 29,30,31]. It is installed on software BEAM like module. Software BEAM was conceived by the European space agency for the treatment, the analysis, visualization, georeferencing satellite images, in particular those produced by ESA (MERIS, AATSR, ASAR, etc). Images AASTR were atmospheric corrected by model SMAC before being used in model SEBS. This model SMAC (Simplified Method for Atmospheric Corrections) is also a module of BEAM developed for the atmospheric correction of images MERIS and AATSR of satellite ENVISAT. The practical application of SMAC is to change the equation of radiative transfer, and to calculate the reflectance of surface of satellite measurements.

Model SEBS consists of a whole of tools for the determination of the physical properties of surface of the ground and the variables of state, such as emissivity, the albedo, the temperature and vegetable cover.

Based on contrast between the dry and wet zones, model SEBS was initiated by [19] which proposed a method to calculate the evapotranspiration starting from the evaporative fraction. This concept was improved by [30, 31] to establish model SEBS. To reach the temperature of surface, model SEBS bases emissivities derived and the temperature from brightness of the bands (in Brightness Temperaure) to calculate the land surface temperature through the technique of Split Window (SPT). The advantage of these techniques of Split Window is the elimination of the effects of the atmosphere, except the atmospheric water columns.
Several coefficients of calibration for the technique of Split Window are tested, model SEBS adopts for satellite images AATSR of satellite ENVISAT of the European space agency that of [26, 27, 28].
It should be noted that the study related to 21 pluviometric stations left again well on the catchment area of Kolondieba-Tiendaga

2.3.1 Estimation of the components of the energy assessment
The data of remote sensing and weather are used to calculate the heat flows of surface. Clear radiation is divided into heat flow latent, significant heat flow and heat flow of the ground. The latent heat flow is calculated like a residue of the energy assessment according to the following equation.

$$LE = R_n - G - H$$

Where R_n is clear radiation resulting respectively from the assessment of radiation entering and outgoing (W/m^2)
LE: latent heat flux (W/m^2)
G: heat flux of the ground (W/m^2)
H: Sensible heat (W/m^2)
R_n and G can be estimated locally by using weather data [1] and on a regional level by incorporation of emitted and reflected radiation distributed spatially[14,15].
Net radiation (R_n). The assessment of radiation of the surface of the ground is given by the following formula.

$$R_n = R_{s\downarrow} - R_{s\uparrow} + R_{L\downarrow} - R_{L\uparrow}$$

Where

R_n :Net radiation

$R_{s\downarrow}$: radiation short wavelength (0,14-4µm) coming from the sun

$R_{s\uparrow}$: radiation big wavelength) (>4µm) coming from the atmosphere

$R_{L\downarrow}$: Quantity of radiation emitted by terrestrial surface

$R_{L\uparrow}$; Quantity of energy reflected by terrestrial surface

$R_{s\downarrow}$ is calculated starting from the product of instantaneous radiation arriving on the ground,[24]. The solar radiation absorptive by surface of the ground is calculated according to the following relation:

$$R_{abs} = (1-\alpha) R_{s\downarrow}$$

Where α is the albedo of surface. It is given starting from measurement of narrow bands by the technique of average of weight suggested by [27]. The radiation arriving big length $R_{L\downarrow}$ is estimated starting from measurements on the ground of the temperature of the air and the steam pressure by using the following relation:

$$R_{L\downarrow} = \varepsilon_a \sigma R_a^4$$

Where is the emissivity of the atmosphere $\left[\varepsilon_a = 1{,}24 \left(e_d / T_a \right)^{1/7} \right]$, σ is the constant of Stefan-Boltzmann (5, $67x10^{-8} W/mk^{-4}$, your is the temperature of the air in (K) and e_d is the deficit of pressure in (mbar). The radiation big wavelength leaving ($R_{L\downarrow}$) is obtained starting from the temperature of surface by being unaware of the small contribution of the radiation of the sky reflected by using the following equation:

$$R_{L\uparrow} = \varepsilon_s \sigma T_s^4$$

Where ε_s is the emissivity of surface and is the temperature of surface (°K). According to [31], emissivity (εs) for the range of 8-14µm could be predicted starting from the NDVI with a strong correlation. Emissivity (ε_s), is thus calculated starting from the NDVI by using the relation following logarithmic curve:

$$\varepsilon_s = 1{,}0094 + 0{,}047 x \ln(NDVI)$$

The quantity of clear radiation received by surface is the entering and leaving sum of all radiations and is calculated according to the equation below.

$$R_n = (1-\alpha) R_{s\downarrow} + \varepsilon_a \sigma T_a^4 - \varepsilon_s T_s^4$$

2.3.1.1 Heat flux of the ground (G): The heat flux of the ground (G) is commonly considered like a fraction of clear radiation R_n depending on the index of the leaf area Index (LAI) and the NDVI (Normalize Vegetation Index) [11]. It can be higher than $0{,}3R_n$ for the grounds naked and lower than 0,1Rn for the covered zones of vegetation [14,15]. Several studies showed that the G/R_n ratio of the day is relative to other factors, such as the quantity of vegetation present [2, 3, 18, 10] presented the following relation to estimate the heat flow of the ground G.

$$G = R_n \left(\frac{T_s}{\alpha} \right) x \left(0{,}0038\alpha + 0{,}0074\alpha^2 \right) x \left(1 - 0{,}98\, NDVI^4 \right)$$

2.3.1.2 Sensible flux heat (H): The estimate of the reliable values of significant heat flow is the most difficult aspect of this methodology because it depends on aerodynamic resistance. H is commonly expressed like a function of T_s and T_a.

$$H = \rho C_p (T_s - T_a) / r_a$$

Where ρ is the density of the dry air (Kgm^{-3}), C_P is the capacity of specific heat of the air ($Jkg^{-1}C^{-1}$), and r_a is the aerodynamic resistance of the transport of heat (s/m^{-1}). r_a is estimated by the theory of similarity of Monin-Obukhov [5]. Many models semi-empirical were proposed to estimate r_a and H [6, 33, 34]. Among these models, that presented by [6], proposes simplest to estimate H starting from some points of measurement easily obtained, such as the NDVI, T_s and T_a. The principal problem of this method is the over-estimate of H in urban environment where the index of vegetation is weak from where an over-estimate of [25].

To avoid this problem a model of aerodynamic resistance semi-empirical was proposed by [33].

$$r_a = 4{,}72 \left\{ \ln(z / z_0) \right\}^2 / (1 + 0{,}54u)$$

Where z is the height the speed of the wind (m), z_0 is the length of roughness of surface (m) and u is the speed of wind (m/s^{-1}).

[13, 21] showed that z_0 can be estimated starting from index of vegetation, such as the NDVI and the ratio of NIR/R. [10] also connected z_0 (cm) with the NDVI to estimate flux of surface at the regional level.[21] used an exponential relation to estimate z_0 starting from ratio NIR/R

$$Z_0 = \exp(0{,}01021 + 0{,}1484(NIR / \mathrm{Re}\, d))$$

2.3.1.3 Estimation of land surface temperature

As announced higher, the temperature of surface was estimated according to the formula of [26], was integrated directly in module SEBS of BEAM. This formula is based on the temperature of brightness, the steam contents, the emissivity of surface and the difference in emissivity to calculate the temperature of surface of the ground

$$LST = 0{,}39T_1^2 + 2{,}34T_1 - 0{,}78T_1 x T_2 - 1{,}34T_2 + 0{,}39T_2^2 + 0{,}56$$

Where T1 and T2 represent respectively bands 6 and 7. The coefficients are empirically given on the basis of type of occupation of the ground, vegetable cover, the season and the duration of the day, the atmospheric steam pressure, the zenith angle and the emissivity of surface [23]

3. Results and Discussion

3.1 Space-time distribution of the values of temperature of surface of 2003 to 2010 analyzes

From the analysis of the **tableau3**, it appears that the median values of the temperatures of surface of the ground estimated starting from satellite images AATSR, using model SEBS (Surface Energy Balance System), on the catchment area of kolondièba-Tiendaga, oscillate between 300 and 292°K. At the same time, the maximum and minimal values vary respectively between 303 and 299°k (maximum values) and between 288 and 299°K for the minimal values.

As for the values of standard deviation, they vary between 1 and 3.

In addition, we found that the highest values of temperature of surface were recorded respectively into 2007,2003,2005,2006,2010,2009,2004 where they vary between 303 and 299 (°K). On the other hand, the low value estimated during this study was recorded in 2008 (296°K). These values are in the same fork as those found by [23], on the basin of Volta, in West Africa with the same types of satellite data (AASTR.)

The analysis of the space-time variation between 2003 and 2010 revealed that the year 2007 is hottest with the value of temperature of the highest surface (303°K) for a standard deviation of 2,67. Whereas year 2008 is shown the least hot, where 296,21°K was estimated with a standard deviation of 0,945.

It should however be recognized that these results were not validated, because of the limited means. Indeed, the project did not have average materials sufficiently to undertake studies of validation of ground.
The analysis of the various charts worked out starting from these values of temperature of surface of the ground shows that these values increase South in North, contrary to those of the evapotranspiration, over the same study period (2003 to 2010), under the same conditions.
Indeed, we noticed that the values of temperatures of surfaces of the ground are high on the parts of the catchment area where the percentage of naked ground is most important. While the low values of temperatures of surface of the ground are observed in the zones where vegetable cover is relatively much more important, and richer in hydrographic terms of networks and water resource.
We can conclude that the variation of the median values of temperature of surface on the catchment area of Kolondièba-Tiendaga, in southern Mali zone, follows the dynamics of occupation of the grounds.
Table 3: Comparaison des valeurs de température de surface mesurées (°K) à partir des images AATSR de 2003 - 2010 sur le Bassin versant de Kolondièba-Tiendaga

Stations	2003	2004	2005	2006	2007	2008	2009	2010	Moy	Max	Min	Std variat
1	296,92	293,17	295,10	298,94	295,39	295,67	291,48	290,96	294,70	298,94	290,96	2,70
2	299,06	294,13	294,58	296,14	297,29	295,22	291,65	294,81	295,36	299,06	291,65	2,21
3	298,57	296,31	296,23	295,59	296,69	295,66	292,68	292,51	295,53	298,57	292,51	2,03
4	297,57	297,77	297,72	296,02	298,86	296,18	292,63	291,16	295,99	298,86	291,16	2,71
5	298,19	298,25	297,82	296,69	296,61	295,67	293,83	291,59	296,33	298,25	291,59	2,16
6	299,84	297,61	298,42	296,94	295,35	292,90	296,71	292,66	296,30	299,84	292,66	2,54
7	302,50	297,45	297,24	295,40	295,23	296,04	298,56	291,57	296,75	302,50	291,57	3,13
8	301,92	297,18	296,03	293,49	293,61	295,17	296,80	291,49	295,71	301,92	291,49	3,15
9	301,80	298,62	298,16	297,15	295,89	296,14	291,88	298,10	297,22	301,80	291,88	2,83
10	300,69	296,12	298,82	298,82	297,31	294,84	290,88	295,70	296,65	300,69	290,88	3,02
11	298,52	296,31	299,52	299,13	297,95	295,58	292,61	298,47	297,26	299,52	292,61	2,31
12	298,23	294,65	297,64	297,83	300,01	293,58	293,69	297,69	296,66	300,01	293,58	2,37
13	299,73	296,44	298,67	299,73	300,48	295,92	294,05	297,59	297,83	300,48	294,05	2,23
14	302,80	295,44	298,51	295,30	300,59	295,72	290,76	298,66	297,22	302,80	290,76	3,72
16	301,28	296,39	298,02	299,48	300,00	294,44	290,12	298,65	297,30	301,28	290,12	3,60
15	302,83	295,89	296,83	297,24	302,20	294,22	290,46	296,75	297,05	302,83	290,46	4,02
18	300,63	291,70	295,36	299,37	300,76	294,36	288,54	297,36	296,01	300,76	288,54	4,38
17	301,56	293,89	298,74	293,33	298,94	294,44	290,94	297,84	296,21	301,56	290,94	3,58
19	298,19	291,50	298,25	295,17	301,29	293,76	288,88	298,76	295,73	301,29	288,88	4,17
20	299,87	293,94	298,65	295,49	303,49	295,60	291,63	299,88	297,42	303,49	291,63	3,83
21	299,30	293,48	297,47	294,78	301,05	296,09	289,97	300,26	296,55	301,05	289,97	3,75
Moy	300,00	295,54	297,51	296,76	298,52	295,10	292,42	295,83				
Max	302,83	298,62	299,52	299,73	303,49	296,18	298,56	299,88				
Min	296,92	291,50	294,58	293,33	293,61	292,90	288,54	290,96				
Std variat	1,80023	2,0569	1,35218	1,9491	2,666	0,9446	2,6806	3,23242				

3.2 Analyzes correlation between the temperature of surface and the indices of vegetation (NDVI)

Front, to carry out this analysis, we thought necessary to have the advantages and the limits of the NDVI.
Defines by [26], the NDVI is the index of vegetation most frequently used in the studies on the follow-up of the vegetation, and is admitted by the whole of the scientific community as being most reliable. This index gives an account of the chlorophyllian activity of canopy and makes it possible to quantify the produced vegetable biomass [26]. The applications of the NDVI are numerous: evaluation of deforestation, follow-up of forest fires, the turning into a desert and same of the devastations caused by insects [26].
Given that the vegetation absorbs an important part of the solar radiation in the red and that it reflects it in the infra-red close relation, its formula can be written

$$NDVI = \frac{\rho_{NIR} - \rho_{R}}{\rho_{NIR} + \rho_{R}}$$

Where

ρ_{NIR} is the spectral band corresponding to the infra-red close relation (ranging between 0,55 and 0,68 µm)

ρ_{R} that corresponding to the red (including between 0,73 and 1,1µm). The theoretical values of the NDVI vary [26] consider that this index is sufficiently stable between -1 and 1 (between 0,1 and 0,9 for the vegetation).
toallowcomparisons of the vegetable activity steps seasonal or interannual times. They add that the force of the NDVI even lies in its design. Indeed, this index being a ratio, calculated starting from two spectral bands, it makes it possible to eliminate part of certain noises like the atmospheric contaminations (aerosols…), differences in illumination of the ground or shade cloudy. In addition, the NDVI has an interesting resolving power: the clouds, water, and snow have a greater reflectance in the visible one in the infra-red, their NDVI is thus negative and one can insolate them easily. Contrary, the naked rocks and grounds will have a similar reflectance in the visible one and the infra-red close relation, but their very low value of NDVI, on both sides of zero, does not allow confusion with vegetation [26].This index has only advantages, [26, 37] recognize some limiting with the NDVI. In particular the recurring presence of atmospheric contaminations residual or of skews related on the camera angle and the relief. Its principal disadvantage is its tendency to saturation when the foliar density (LAI) is too strong on the level of the groundThe index saturates and accounts more for the phenologic variations so covered vegetable is too dense It arises from the analysis between the monthly values of temperature of surface (LST) and the index of vegetation (NDVI) which it exists a strong correlation between the two parameters. Indeed, our results show strong values

coefficients of correlation for the years (2005, 2004, 2007, 2006, 2003). We respectively obtained values of R2 (0,834; 0,716; 0,686; 0,582; 0,563). On the other hand, a low coefficient of correlation is observed for the years (2008, 2009, 2010), where respective values of R^2 (0,394; 0,376; 0,178) are obtained. The fall of R^2 for these years is explained by the lack of data for years. Indeed, for these three years. There were less data AATSR, in particular for the months from July-August. This insufficiency of data can be at the origin of this fall.

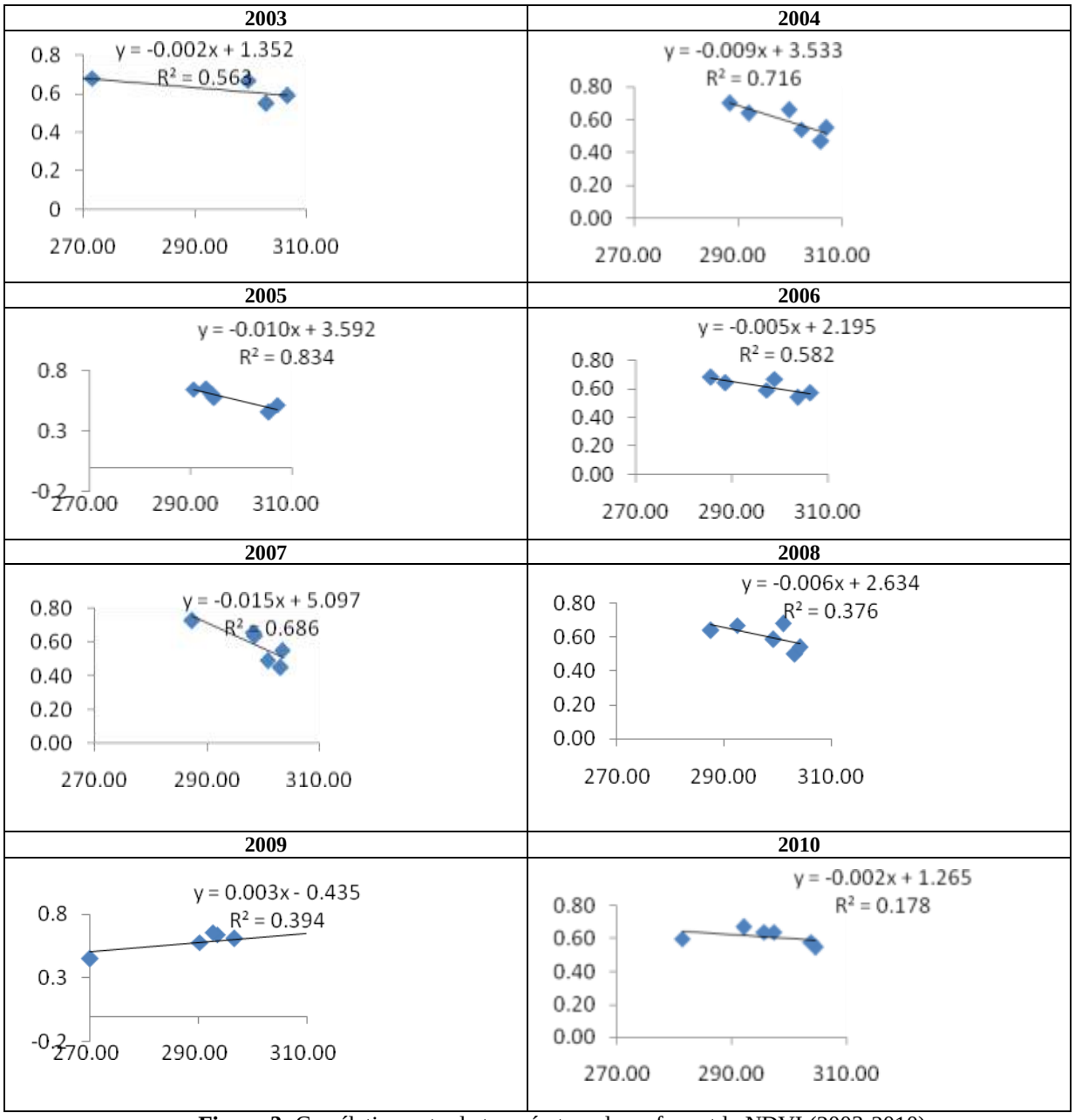

Figure 3: Corrélation entre la température de surface et le NDVI (2003-2010)

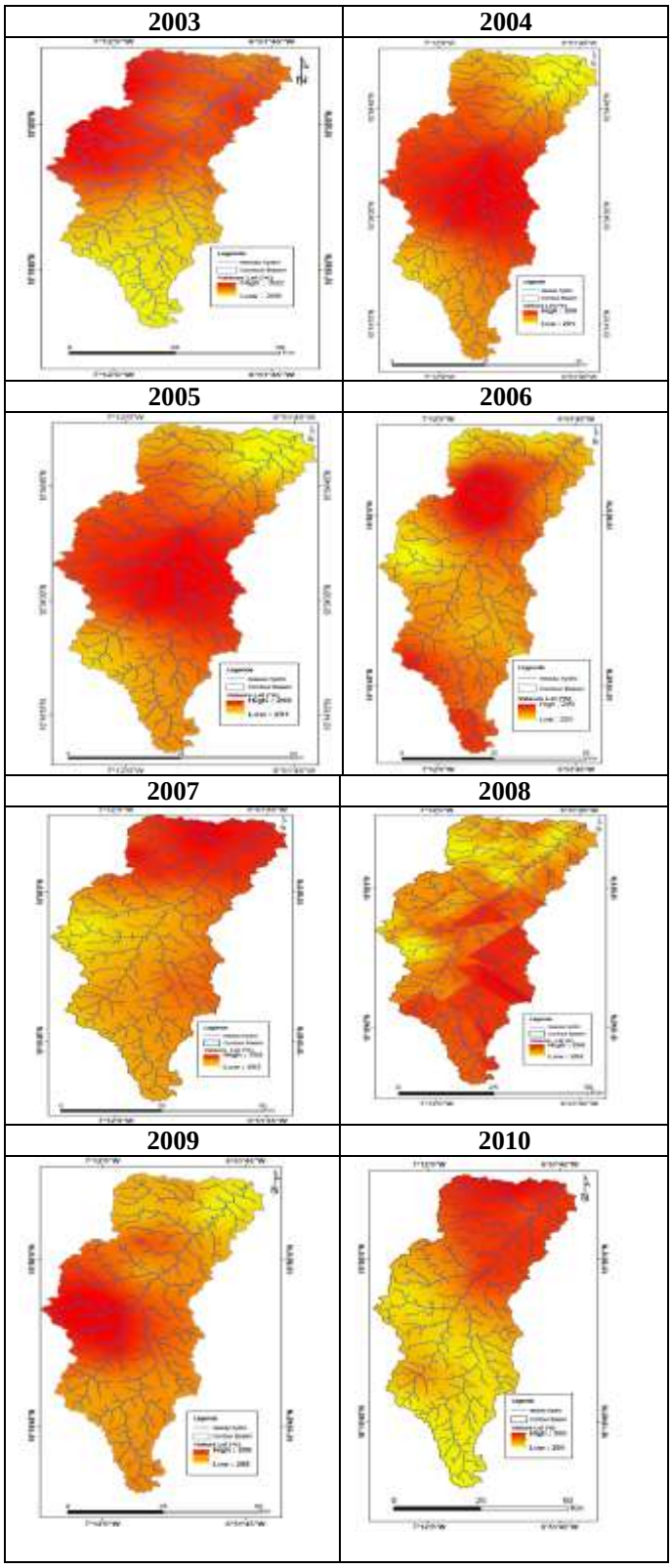

Figure 4: Charts of temperature of surface (°K) of the catchment area of Kolondièba-Tiendaga between 2003 and 2010 elaborate starting from images AATSR

4. Conclusion

The tools for remote sensing and GIS appear today like an essential element in the collection and the mapping of the parameters biophysics on broad scales, of which in particular the evapotranspiration, the land surface temperature, emissivity, albedo, etc

The use of model SEBS developed by [31] made it possible to determine and chart the temperature of surface starting from satellite images AATSR on the catchment area of Kolondièba-Tiendaga in climate soudano-saheliaen, in southern the Mali zone. The results obtained of the study show values of temperature which vary between 303 and 296 with standard deviations of (2,66 and 0,945). These same results show a very good tendency with the evapotranspiration calculated starting from the evaporative fraction.

For the later studies, it would be more adapted to make a comparison between the values of temperature of surface estimated starting from model SEBS and those collected starting from a station or a measuring device of land surface temperature.

Acknowledgement

Our thanks are addressed to DANIDA for the financial support of this study within the framework of project WANSEC (West African Network for Studies Environment Changes). Our thanks are also addressed to the European space agency (ESA) for its customer support within the framework of project TIGER II.

We thank the Eau unit and Environment for the DER of Geology of the ENI-ABT of Bamako (Mali) to have sheltered this work.

In end, we thank the IRD through project RIPIECSA for its support in the finalization for the drafting for this article.

References

[1] Allen,R., Pereira, L., Raes, D., Smith, M., (1998). Crop evapotranspiration guidelines for computing crop water requirements. FAO Irrigation and Drainage Paper, 56. FAO, Rome.

[2] Bastiaanssen, W.G.M., (2000). SEBAL based sensible and latent heat flux in the irrigated Gediz Basin, Turkey. Journal of hydrology, 229, pp. 87-100

[3] Bastiaanssen, W.G.M., Menenti, M., Fedds, R.A. and Holtslag, A. A. M., (1998). A remote sensing surface energy balance algorithm for Land (SEBAL)-1. Formulation. Journal of hydrology, 212/213, pp. 198-212

[4] Bhattacharya, B. K., Dadhwal, V.K., (2003). Retrieval and Validation of land surface temperature (LST) from NOAA AVHRR thermal images of Gujarat , India. International Journal of Remote sensing, 24,06,pp. 1197-1206

[5] Businger, J.A. (1988). A note on the Businger Dyer profiles. Boundary- Layer Meteorological, 42: 145 151.

[6] Carlson, T. N., Capehart, W.J., and Gillies, R.R., (1995). A new look at the simplified method for remote sensing daily evapotranspiration. Remote sensing of Environment. 54, 2, pp. 161-167.

[7] Chen, D., Gao, G., Yu, C. Y., Guo, J., Ren, G., (2005). Comparison of the thornthwaite method and pan data with the standard Penman-Monteith estimates of references evapotranspiration in China. Climate Research, 28, pp. 123-132

[8] Courault, D., Seguin, B., Olioso, A., (2005). Review on estimation evapotranspiration from remote sensing data: from empirical to numerical modeling approaches. SPRINGER. Irrigation and Drainage system, 19, pp. 223-249

[9] French, A. N., Schmugge, T. J., kustas, W. P., Brubaker, K. L., et Prueger, J., (2003). Surface energy fluxes over EL Reno Oklahoma, using high resolution remotely sensed data. Water resources research 39(6), 1164

[10] Gao, W., Coulter, R. L., Lesht, B. M., Qui, J., Wesley, M. L., (1998). Estimating clear-sky regional surface fluxes in the southern great plains atmospheric radiation measurement site with ground measurement and satellites observations. Journal of Applied Meteorology, 37, pp. 5-22.

[11] Gowda, H.P., Chavez, L. J., Calaizzi, D. P., Evett, R. S., Howell, T. A., Tolk, A. J., (2007). ET mapping for agricultural water management: Present status and Challenges. Springer Verlag, Irrigation Science, 26, pp. 223-237.

[12] Gupta, R. K., Prasad, S., Sesh Sai, and Viswanadham, T. S., (1997). The estimation of land surface temperature over an agricultural area in the state of Haryana and Panjab, India, and its relationships with the Normalized Difference Vegetation Index (NDVI) using NOAA AVHRR data. International Journal of Remote sensing, 18, 18, pp. 3729-3741

[13] Hatfield, J. L., (1988). Large scale evapotranspiration from remotely sensed surface temperature in proceedings: planning now for irrigation and drainage, Lincoln NE, 18-21 July, American Society of Civil Engineers (ASCE). New York, pp. P205-P509.

[14] Jacob, F., Oliosio, A., Gu, X., Su, Z., & Seguin, B., (2002a). Mapping surface fluxes using airborne, visible, near infrared, thermal infrared remote sensing and a spatialized surface energy balance model. Agronomie, 22, 669-680

[15] Jacob, F., Schmugge, T., Ogawa, K. A. F., & Ritchie, J., (2002b). The potentialities of ASTER to retrieve radiative properties over semi arid regions. In J. Sobrino (Ed), First International Symposium on recent advances in quantitative remote sensing, pp. 913-920

[16] Jia, L., Su, Z., Van den Hurk, B., Menenti, M., Moene, A., De Bruin H. A. R ., Yrissary, J. J. B., Ibanez, M., and Cuesta, A., (2003). Estimation of sensible heat flux using the Surface Energy Balance System (SEBS) and ASTER measurements. Physics Chemistry of the Earth, 28(1-3), 75-88

[17] Kant, Y., Badarinath, K. V. S., (2000). Studies of land surface temperature over heterogeneous area using AVHRR data. International Journal of Remote sensing, 21, 8, pp, 1749-1756

[18] Kustas, W. P., and Norman, J. M., (1999). Reply to comments about the basic equations of dual-source vegetation-atmosphere transfer models. Agricultural and Forest Meteorology, 94, 275-278.

[19] Menenti, M., Choudhury, B. J., (1993). Parameterization of land surface evapotranspiration using a location dependent potential evapotranspiration and surface temperature range. In: Boll, A.J. et al., (eds) Proceedings of exchange of processes of land surface for the range of space and time scales. IAHS Publ 212, pp. 561-568.

[20 Menenti, M., Jial, L., Su, Z., (2003). On SEBI-SEBS validation in France, Italy, Spain, USA, and China. In: Co-chair Allen, R. G., Bastiaanssen, W., (eds) Proceedings of the workshop on use of remote sensing of crop evapotranspiration for large regions. International Commission on Irrigation and Drainage (ICID) Monptellier

[21] Moran, M. S., (1990). A satellite based approach for evaluation of the spatial distribution of evapotranspiration from agricultural lands (dissertation abstract). PhD dissertation, University of Arizona, Tuscan.

[22] Norman. J. M., Kustas, W. P., Humes, K. S., (1995). A two- sources approach for estimating soil and vegetation energy fluxes from observation of directional radiometric surface temperature. Agric for Meteorol 77, 263-293

[23] Opoku Duah, S., Donoghue, D. N. M., Burt, T .P., (2008). Intercomparison of evapotranspiration over the Savannah Volta Basin in West Africa using remote sensing data. SENSORS.ISSN, 1424-8220

[24] Parodi, G. N., (2000). AHVRR Hydrogical Analysis System, Algorithms and theory- Version 1.0. International Institute for Aerospace and Earth Science (ITC), Wageningen, the Netherlands.

[25] Richter, R., (2002). ATCOR for ERDAS imagine (Ver. 2.0). Manual User. Geosystems GmbH, Riesstr, 10, D-82110 Germering, Germany.

[26] Rousse, J.W., Haas, R.H., Schell, J.A., and Deering, D.W. (1973). Monitoring vegetation systems in the great plains with ERTS. In ERTS Symposium, NASA, SP-351, Washington DC, vol. 1, pp. 309-317.

[27] Sarwar, A., Bill, R., (2007). Mapping evapotranspiration in the Indus basin using ASTER data. International journal of remote sensing, 28, pp. 5037-5047

[28] Sobrino, J.A., Gomez, M., Jiménes-Munos, J. C., Olioso, A., (2007). Application of a simple algorithm to estimate daily evapotranspiration from NOAA-AVHRR images for the Liberian Peninsula. Remote sensing of Environment, 110, pp. 139-148

[29] Sobrino, J. A., Jiménez Munoz, L. C., (2005). Land surface temperature retrieval from thermal infrared data: An assessment in the context of the surface processes and ecosystem changes through response analysis (SPECTRA) mission, Journal of Geophysic al Research, 110, D16103, doi: 10. 1029/2004JD005588

[30] Su, Z., Pelgrum, H., and Menenti, M., (1999). Aggregation effects of surface heterogeneity in land surface processes. Hydrology and Eartth System Science, 3 (4), 549-563.

[31] Su, Z., Schmugger, T., Kustas, W. P., Massman, W. J., (2001). An evaluation two models for estimation of the roughness height for heat transfer between the land surface and atmosphere, J, Appl Meteorol, 40, 1933-1951

[32] Su, Z., (2002). The surface energy balance system (SEBS) for estimation of the turbulent heat fluxes. Hydrology and Earth Science, 6(1), 85-99

[33] Thom, A.S., and Oliver, H.R., (1977). On penman's equation for estimating regional evaporation. Quartely. Journal of the Royal Meteorological Society. 103, 436, pp. 345-357

[34] Viney, N.R., (1991). An empirical expression for aerodynamic resistance in the unstable boundary layer. Boundary Layer Meteorology. 56, 4, pp. 381-393.

[35] Wang, K., Wang, P., Li, Z., Cribb, M., & Sparrow, M., (2007). A simple method to estimate actual evapotranspiration from a combination of net radiation, vegetation index, and temperature. Journal of Geophysical research, 112, pp. D15107

[36] Wanger, W., (1998). Soil moisture retrieval from ERS scatterometer data. PhD dissertation to the technisch-naturwissenschaftliche fatkultät of the Vienna University of Technology, Karlsplatz, 13, A 1040 Wien Austria

[37] Zhang, J., Wang, Y., Wang, Z., (2007). Change analysis of land surface temperature based on robust statistics in the estuarine area of Peark River (China) from 1990 to 2000 by Landsat TM/EMT+ data. International Journal of remote sensing, 28, 10, 2383-2390